Micropaleontological Investigations of Pacific Manganese Nodules

AUTHOR(S):

Harada, Kenichi

CITATION:

Harada, Kenichi. Micropaleontological Investigations of Pacific Manganese Nodules. Memoirs of the Faculty of Science, Kyoto University. Series of geology and mineralogy 1978, 45(1): 111-132

ISSUE DATE:

1978-07-31

URL:

http://hdl.handle.net/2433/186624

MEMOIRS OF THE FACULTY OF SCIENCE, KYOTO UNIVERSITY, SERIES OF GEOL. & MINERAL.,
Vol. XLV, No. 1, pp. 111–132, Pls. 3–13, 1978

Micropaleontologic Investigation of Pacific Manganese Nodules

By

Kenichi HARADA*

(Received May 17, 1977; Accepted September 9, 1977)

Abstract

Micropaleontologic methods have been applied to the study of external and internal structures of Pacific manganese nodules from a few locations. Acid treatment extracted various types of microfossils from the nodules. Direct observations by scanning electron microscope (SEM) confirmed the universal occurrence of microfossils inside of nodule layers, which enabled the biostratigraphic dating of nodules. The SEM observation of nodules and their acid insoluble residues revealed two distinct textures in nodule layers: One was a laminated and appeared to have resulted from the direct precipitation of ferromanganese oxides from sea water, and the other had a massive and chaotic texture in which conspicuous biologic activity was involved.

Introduction

Marine manganese nodules, comprising ferromanganese oxides, occurring on the ocean floor, have been an attractive subject of study for oceanographers since their first discovery during the voyage of H. M. S. *Challenger* (1872–1876) (see GLASBY, 1977). In spite of the accumulation of considerable knowledge on their occurrence, distribution, physical properties, chemical and mineral composition, and accretion rate, their origin still remains the subject of speculation (see HARADA, 1977b). One of the reasons for this is that little attention has been paid to the internal structure of manganese nodules which records their growth history (SOREM, 1967).

I have attempted an examination of the internal structure of Pacific nodules by using micropaleontological methods to obtain the information on their age of formation and growth mechanism. In this article I report the results of micropaleontologic investigation of manganese nodules with different morphology from different environments. I will discuss the potential value of the biostratigraphic dating method established by this work, and will consider the process of nodule formation in terms of their growth mechanisms.

* Present address: Geologisch- Paläontologisches Institut und Museum der Universität Kiel, D-2300 Kiel, West Germany.

Material

The material used in this study were manganese nodules displaying different morphologies from different environments in the Pacific. Table 1 presents several aspects on the nodule samples, and Figure 1 shows sample locations. Sample 1 was collected by dredge at the lower flank of the Komabashi Daini Seamount during the GDP-8 Cruise (SHIKI *et al.*, 1974), and Sample 2 was obtained by dredge from the summit of the Makarov Guyot during the R/V *Hakuho-Maru* KH-74-4 Cruise (NASU, 1978). Sample 3 was provided by Dr. Geoffrey P. GLASBY, New Zealand Oceano-

Table 1. Sample location, nodule type, and type of associated sediments.

Sample #	1	2	3	4
Sample name	GDP-8-12Mn	KH-74-4 (#16002)	G994	GH-74-5 (St. 126)
Locality	29° 55.6'N 133° 18.5'E	29° 25.7'N 153° 27.3'E	22° 56.2'S 162° 04.8'W	09° 30.3'N 167° 03.5'W
Water depth	2,250 m	1,377 m	4,848 m	5,010 m
Sea region	Komabashi Daini Seamount (flank)	Makarov Guyot (summit)	Southwestern Pacific Basin	Eastern Central Pacific Basin
Maximum diameter	9.2 cm	15 cm	5 cm	3 cm
Sediment type	Calcareous ooze	Brown clay	Yellow-brown clay	Siliceous-calcareous ooze

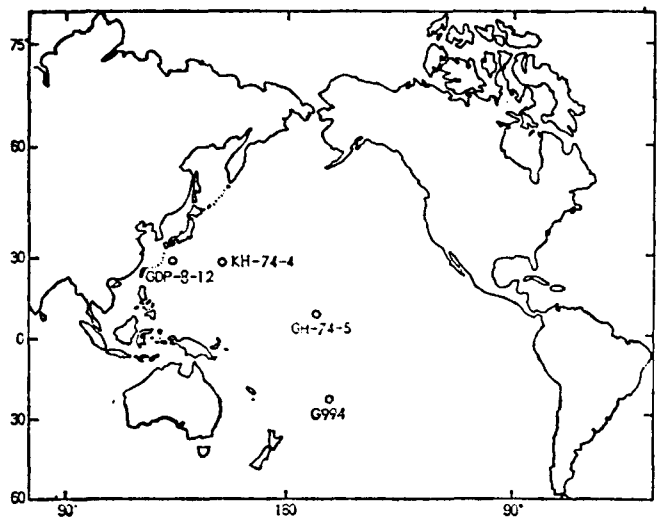

Figure 1. Sample location map.

graphic Institute, who collected it from the Southwestern Pacific Basin during the R/V *Tangaroa* Cruise (MEYLAN *et al.*, 1975), and Sample 4 was supplied by Dr. Atsuyuki MIZUNO, Geological Survey of Japan. It was obtained from the Eastern Central Pacific Basin during the G. S. V. *Hakurei-Maru* GH74-5 Cruise (MIZUNO and CHUJO, 1975). Chemical analyses on the nodules from the Komabashi Daini Seamount and the Southwestern Pacific Basin were performed by USUI *et al.* (1976) and GLASBY *et al.* (1975), respectively.

Methods of Study

The manganese nodules were examined by several micropaleontologic methods. The nodule surface was usually first examined by optical microscope. During the early stages of the study the nodules were washed with dilute hydrochloric acid to remove any calcareous sediment from the surface. As this treatment was found to destroy fine surface textures, however, the untreated surface was observed in later part of the study. Although it is well known that a polished surface of a nodule section presents more a detailed internal structure (SOREM, 1967, 1973), this method was not employed here because of technical difficulties.

The microtexture was studied using scanning electron microscope (SEM). Ferromanganese layers were peeled off by hand along natural boundaries after drying at room temperature. Each layer was placed on a plug after careful trimming so as not to destroy the surface structure, and coated with thin films of carbon and gold in a vacuum evaporator. Some of the trimmed specimens were left in dilute hydrochloric acid solution until they became pure white in color. The insoluble residue was placed on a plug after rinsing with distilled water. As the dried residue is usually very fragile and porous, it is recommended to coat it thickly with carbon under relatively low vacuum condition in the evaporator to ensure a high quality image of SEM.

Siliceous fossils were picked out from the acid insoluble residues. Organic microfossils were extracted by hydrofluoric acid treatment of the residues.

The SEM observations were performed at College of General Education, Osaka University during the early stage of the study, and at Nara University of Education in later part of the study, using a HITACHI-Akashi Minisem and a HITACHI HSM-2B SEMs, respectively.

Results of Observation

1) Sample 1

This specimen is an ellipsoid 92 mm in length and 48 mm across, having an acidic rock fragment as nucleus. The crust, 14 to 20 mm thick, consists of many concentric bands. The surface is covered with botryoids 0.5 to 1 mm in diameter. The nodule

Table 2. Planktonic foraminiferal assemblage and calcareous nannoplankton assemblage in the ooze obtained with sample 1.

Globorotalia (G.) tumida plesiotumida
Sphaeroidinellopsis seminulina seminulina
S. seminulina kochi
S. subdehiscens
Globigerina nepenthes
Ceratolithus tricorniculatus
Discoaster asymmetricus
D. brouweri
D. challengeri
D. surculus
D. variabilis
Reticulofenestra pseudoumbilica
Sphenolithus abies

After HARADA *et al.*, 1974

was associated with calcareous ooze which was composed mainly of Pliocene microfossils (Table 2) (HARADA *et al.*, 1974). However, the planktonic foraminifers incorporated at the surface with the botryoids of ferromanganese oxides are such Pleistocene species as *Globorotalia menardii* (D'ORBIGNY), *G. truncatulinoides* (D'ORBIGNY), *G. inflata* (D'ORBIGNY), and *Pulleniatina obliqueloculata* (PARKER *et* JONES). Small tubes, less than 0.3 mm in diameter, were found, but no sessile foraminifers were discovered. The tubes were usually covered with black ferromanganese oxides.

SEM observations revealed numerous calcareous nannoplankton fossils preserved as impressions inside of the crust (Pl. 3, figs. a–f). Their distribution was not uniform. They were abundant in the parts of coarse texture, and scarce in those of laminated and dense texture (Pl. 5, fig. h). Although the preservation was poor, three species were identified; *Coccolithus pelagicus* (WALLICH) SCHILLER, *Cyclococcolithina macintyrei* BUKRY *et* BRAMLETTE, and *Umbilicosphaera mirabilis* LOHMANN (Pl. 3, figs. b, d, e). Members of *Discoaster* were not recognized. Planktonic foraminiferal tests were commonly observed. As they were preserved as impressions (Pl. 4, fig. g), or were replaced by ferromanganese oxides (Pl. 4, fig. h), specific identification was not possible. In addition to the planktonic microfossils, a colony of small particles were discovered in a certain place (Pl. 3, figs. g, h).

Surface of the inner layers usually has a botryoidal surface similar to the nodule surface (Pl. 4, fig. e). This feature was observed commonly in the other nodules (Pl. 7, fig. g; Pl. 12, fig. h). It is considered to be preserved ancient growth surface as has been suggested by FEWKES (1973).

The acid treatments extracted various microfossils. Fragments of sponges and radiolarians, and cores of planktonic foramnifers were found in hydrochloric acid

residue. From the organic remains after hydrofluoric acid treatment, several kinds of scales of butterfly were discovered (Pl. 4, figs. a-d). Since they were extracted twice from the single specimen abundantly during mid winter, they are considered not to be contaminants during the process, although their stratigraphic position in the crust has not been determined. A few pollen grains and spores were also extracted, but no dinoflagellate cyst was discovered.

2) Sample 2

This sample is a spheroid about 15 cm in diameter, having small bumps on the surface, and is the largest specimen. The calcareous nannoplankton assemblage found on the surface (Pl. 5, fig. d) indicates that it is Recent in age. Small tubes covered with nannofossils were observed (Pl. 5, figs. a, b). A benthic foraminifer was found on the surface (Pl. 5, fig. c). Like Sample 1, numerous calcareous nannoplankton fossils were discovered inside. As the preservation was better than in the previous case, more species were identified; *Coccolithus pelagicus*, *Cyclococcolithina leptopora* (MURRAY *et* BLACKMAN) KAMPTNER, *Cycl. macintyrei*, *Gephyrocapsa oceanica* KAMPTNER, *Pseudoemiliania lacunosa* (KAMPTNER) GARTNER, and *Umbilicosphaera mirabilis* (Pl. 5, figs. e, f). Three distinct assemblages were recognized at three different places of the crust; the surface, the outermost layer, and the innermost layer adjacent to the nucleus. Although several individuals of *Chiasmolithus grandis* HAY, MOHLER *et* WADE, one of the Eocene index fossils, were discovered in a cavity, they were regarded as reworked fossils judging from their occurrence and appearance (Pl. 5, fig. g). The observations of this specimen have been published in detail by HARADA and NISHIDA (1976).

3) Sample 3

The specimen is a sphere 5 cm in diameter, having a round nucleus of altered volcanic material. The crust, about 20 mm thick, comprises three layers: The outermost layer, 1 mm thick, with botryoidal surface (Pl. 6, figs. a, b); the middle layer, about 4 mm thick, consisting of many thin lamellae in the upper 1 mm; and an innermost layer, about 15 mm thick, massive and dense in texture, containing many white

Table 3. Calcareous nannoplankton assemblage in the sediment obtained with sample 3.

Cyclococcolithina leptopora	42%
Ceratolithus cristatus	37
C. rugosus	3
Gephyrocapsa oceanica	9
Umbilicosphaera mirabilis	7
Pseudoemiliania lacunosa	2

Total counted individuals=228.

inclusions and cavities. The surface of the outermost and intermediate layers presented small hollow tubes (Pl. 6, fig. c; Pl. 7, fig. h). The innermost layer was covered with a veneer of white clay where relatively large broken tubes were found.

The sediment obtained with the nodule at the site of collection contained poorly preserved calcareous nannoplankton fossils. The assemblage, shown in Table 3, indicates NN 19 (Neogene Nannoplankton Zone; MARTINI and WORSLEY, 1970).

The upper two layers were examined using SEM. A few broken hollow tubes (Pl. 6, fig. c) and some filamentous objects (Pl. 6, figs. e, f) were observed. Although the latter existed even in the acid insoluble residue of this layer (Pl. 9, fig. g), it is not clear if it is an *in situ* organism or a contaminant added during the collection and storage. In some parts, numerous small knobs, about 5 μm in diameter, were discovered covering the botryoids (Pl. 6, fig. g), although other parts of the surface were covered with sediment (Pl. 6, fig. d). Under high magnification, the knobs appeared to be amorphous ferromanganese oxides precipitated from sea water (Pl. 7, fig. a). They were aggregated in the form of a plane on the botryoid surface (Pl. 6, fig. h). A tangential section of the botryoids suggests that the colloidal deposits compose a sheet (Pl. 7, figs. b–d), which seems to be a basic unit of the laminated structure that has been previously reported by MARGOLIS and GLASBY (1973) (Pl. 7, figs. e, f).

The surface of the intermediate layer showed knobby texture similar to that of the outermost layer (Pl. 7, fig. g), where broken tubes were also found (Pl. 7, fig. h). The section of the layer exhibited vaguely laminated texture in the upper part, and chaotic one in the lower (Pl. 8, fig. a). The laminated part was dense in texture, and included no fossils, while the lower part showed tabular structure of biologic origin (Pl. 8, fig. b), and contained many cavities in which unidentified benthic microfossils (Pl. 8, figs. c, e, f) were preserved, and authigenic crystals, probably of zeolite group, were growing (Pl. 8, fig. d). In some parts, assemblage of hemispheric particles were observed (Pl. 8, figs. g, h), although their origin was unknown.

Only a small number of poorly preserved planktonic microfossils were discovered by SEM observation. No chronologic information was obtained from the fossils, due to their scarcity and poor preservation.

The textural difference recognized in the layers became clearer when the layers were leached with hydrochloric acid. The insoluble residue of the outermost layer showed the texture resembling the original one, while those of the lower two layers changed into very porous structures (Pl. 9, figs. a, b).

The surface of the acid insoluble residue of the outermost layer appeared massive under SEM, and no traces of biologic activity were recognized (Pl. 9, figs. c, e), although the filamentous object which was encountered on the untreated surface existed (Pl. 9, fig. g). That of the intermediate layer had a similar texture to the previous one (Pl. 10, figs. a, b), but the bottom surface exhibited very porous framework (Pl. 9, fig. d), which appeared to be composed of various hollow tubes (Pl. 9, figs. f, h). The lower

part of the layer contained abundantly planktonic microfossils (Pl. 10, figs. c, d).

The residue of the innermost layer was also very porous, although the dimension of framework was different from that of the bottom surface of the intermediate layer (Pl. 10, figs. e, f). The structure appeared to be constructed by biologic activity. Unlike the intermediate layer, it contained many authigenic minerals, probably zeolites, inside (Pl. 10, fig. g). Besides the larger hollow tubes, many small tubes were recognized (Pl. 10, figs. g, h). In spite of their small dimensions, they are biogenic, since the outer wall was found to be composed of well sorted grains (Pl. 10, fig. h).

4) Sample 4

The specimen is an intergrown type, comprising several hemisphere, and 3 cm in length. It is the smallest sample. Each hemisphere has concentric bands around a nucleus, and the outer a few layers envelop the whole hemispheres. The outermost layer is about 1.5 mm thick, with a smooth surface; and the layer next to it is about 1.7 mm thick.

The surface of the outermost layer was covered with siliceous-calcareous sediment (Pl. 11, fig. b); a few broken hollow tubes were observed (Pl. 11, fig. a). It is noteworthy that calcareous nannoplankton fossils were relatively well preserved in spite of the great water depth (Pl. 11, fig. b). Their assemblage indicates Recent age.

The upper 0.5 mm of the outermost layer consisted of fine lamination (Pl. 11, fig. c). Under a veneer of sediment, the same knobby texture as seen in Sample 3 was discovered on a sheet of the lamination (Pl. 11, fig. d). This sheet could result from colloidal deposition of ferromanganese oxides from sea water. The lower part of the layer was massive and dense, and showed some traces of biologic activity.

The inner surface displayed a different morphology. The major area was occupied by small depressions (Pl. 11, fig. e) which may reflect the surface topography of the subsequent layer. Many natural casts of diatoms and calcareous nannoplankton were preserved on the surface of these depressions (Pl. 11, fig. f). As the preservation was poor, no chronologic data were obtained from the fossils. Another part showed ridge-like structures (Pl. 11, fig. g), which were frequently noticed in the other samples. They appeared to be composed of organic material (Pl. 11, fig. h). They are considered to be a constituent material of the tests of encrusting organisms.

The section of the second layer differed considerably from that of the outermost one (Pl. 12, fig. a). The lower part exhibited no laminated structure, but randomly arcuate layering with organic ridges (Pl. 12, fig. b). The upper 0.3 mm of the layer showed aggregation of small particles without the ridge-like structure (Pl. 12, figs. c, d). The particles seemed to be connected with membraneous material (Pl. 12, figs. e, f). Casts of diatoms and calcareous nannoplankton were found in the lower part of the layer.

The surface of the layer was knobby with a smooth surface as seen in the other samples (Pl. 12, figs. g, h). This surface also contained natural casts of diatoms. In

addition to these, individual diatoms and calcareous nannoplankton fossils were seen adhering to the surface (Pl. 13, figs. a, b). The following nannoplankton species were identified; *Cyclococcolithina leptopora*, *Pseudoemiliania lacunosa*, and *Gephyrocapsa oceanica*. Among them, *Cycl. leptopora* was predominant. It suggests that the assemblage belongs to NN 19.

The acid insoluble residue of the layer displayed the same texture as seen in the counterparts of Sample 3. The surface of the outermost layer was rather massive (Pl. 13, fig. c), and showed no indication of biologic activity (Pl. 13, fig. d). It contained, however, many more siliceous fossils than did Sample 3, reflecting the nature of the sorrounding sediment. The residue of the second layer was very porous (Pl. 13, fig. e), and appeared to be constructed by encrusting organisms (Pl. 13, fig. f). The lining of a broken tube was smooth (Pl. 13, fig. g), and composed of small plates (Pl. 13, fig. h), indicating biologic origin. The dimensions of the framework were also different from those found in Sample 3.

Results of the above observations may be summarized as follows.

1) The surface of the nodules commonly exhibits various kinds of small hollow tubes of benthic microorganisms. No agglutinating foraminifers have been identified to date despite previous reports of the occurrence of such species on nodule surface as *Glomospira*, *Placopsilina*, *Rhabdammina*, *Saccorhiza*, and *Tolypammina* (GREENSLATE, 1974a; WENDT, 1974; DUGOLINSKY *et al.*, 1977; SCHAAF *et al.*, 1977).

2) The tubes are usually covered with ferromanganese oxides. They do not, however, appear to accumulate micronodules to form outer walls as has been reported by GREENSLATE (1974b). In the case of Sample 1, a larger foraminiferal test was apparently covered with ferromanganese oxides.

3) All the nodules examined contained various microfossils inside as revealed by acid treatment, they were fragments of siliceous fossils and inner moulds of planktonic foraminifers. Organic fossils such as pollen grains, spores and scales of butterflies were extracted from Sample 1. SEM observation disclosed the presence of fossils of unidentified benthic microorganisms as well as of planktonic ones.

4) The fossil and mineral grain contents are apparently controlled by the associated sediment type. Siliceous fossils are not considered to be of genetic importance, except in Sample 4, despite the previous inferrence made by GREENSLATE (1974b).

5) In addition to the above mentioned fossils, aggregations of small particles of various kinds, less than a few micrometers in diameter, were commonly observed. Judging from the fact that various micro-benthic organisms live on nodules, and that several kinds of bacteria have been extracted from nodules (see EHRLICH, 1975), and in fact *in situ* bacterial colonies were observed on fresh nodule surfaces (LAROCK and EHRLICH, 1975), they may be considered fossil bacterial colonies.

6) Among the microfossils preserved inside the nodules, calcareous nannoplankton fossils are most common and abundant, and of chronologic significance. They are usually preserved as impressions, hence can be regarded *in situ* fossils. As the nodule grows layer by layer with time (SOREM, 1967), the concepts of stratigraphy can be applied to the crust of nodules (SOREM and FOSTER, 1972). Nannofossil zones were recognized in the different layers of Sample 2 (HARADA and NISHIDA, 1976). Although no biostratigraphic zones have been established in Sample 1 and Sample 4, the calcareous nannoplankton assemblages indicated an early-to-middle Pleistocene age for these nodules.

7) In addition to the presence of microfossils, SEM observations have revealed two distinct textures in nodule crust. One is a laminated structure which was first described by MARGOLIS and GLASBY (1973), and the other is a massive and chaotic. The former is typically seen in the outermost layers of Sample 3 and Sample 4, and the latter in the inner layers of these samples.

8) Under higher magnification studies, the surface of Sample 3 seems to comprise a large number of botryoids whose surface was covered with numerous small knobs, about 5 μm in diameter. These appear to be amorphous ferromanganese oxides precipitated from sea water. A tangential section of the botryoids suggests that the colloidal deposits aggregated to form a thin sheet, which is a basic unit of the finely laminated structure. This part seldom contains microfossils. The same feature was observed in the outermost layer of Sample 4.

9) The inner layers of Sample 3 and Sample 4 exhibit many characteristic features which indicate biologic activity; arcuate tabular structures, ridge-like structures made of organic materials, many holes penetrating the matrix, and even fossils of benthic microorganisms and fossil bacterial colonies.

10) The textural difference becomes clearer after leaching the two parts with dilute hydrochloric acid solution. The insoluble residue of the laminated part retained the original features, while the other completely changed and showed very porous texture.

11) The former sustained no conspicuous traces of biologic activity, even under high magnification, although Sample 3 contained organic filaments on the surface. On the other hand, the porous framework appeared to be constructed by various hollow tubes of encrusting organisms which usually withstand the hydrochloric acid treatment (DUDLEY, 1976; GREENSLATE, 1974a). It is of genetic importance that the dimensions of the framework differed not only from nodule to nodule, but also among layers within a single nodule.

12) The framework contains large amount of fossils and authigenic minerals, which are incorporated with tubes of encrusting organisms. This mechanism may explain appropriately the abundant occurrence of scales of butterflies from Sample 1, whose deposition to the ocean floor should be a rare event (HARADA, 1977a; HIURA,

1973). The mineral content also varies considerably.

13) The surfaces of inner layers usually display botryoidal texture resembling that of nodule surfaces. They may be preserved ancient growth surfaces, as have been suggested by FEWKES (1973).

Discussion

The micropaleontologic investigations of marine manganese nodules can provide two kinds of informations on their origin; the age of nodule formation, and the mechanism by which they grew. I will discuss the nodule chronology first.

Two principal methods have been employed to estimate the rate of nodule accretion. One method is based on the distribution of radionuclides such as ^{230}Th, ^{231}Pa, and ^{234}U in successive layers of nodules. The other method is to determine the absolute age of nodule nuclei by dating with fission track, K-Ar dating, *etc.* (see KU, 1977). However, each of the two methods has its shortcomings: The former can only be applied to the upper few millimeters of ferromanganese layers because of the short half-lives of the available nuclides. The latter generally only gives a minimum mean growth rate for the oxide parts of the nodules. Consequently, the age, or growth rate, of intermediate layers of nodules has not been previously determined.

In situ microfossils preserved within marine manganese nodules offer a new method for nodule dating. As the concept of biostratigraphy is applicable to ferromanganese layers, in principle we can determine the age based on a biochronologic scale. Based on the three biostratigraphic zones recognized in Sample 2, two rates of accretion have been obtained for different parts of the nodule; 1–6.7 mm/10^6 yrs for the uppermost layer, and 39 mm/10^6 yrs for the rest as minimum mean growth rate (HARADA and NISHIDA, 1976). The differences in accretion rates may indicate discontinuous growth of the nodule, which has not been demonstrated by the previous methods. The growth history will be clarified by examining accumulation rates by applying the three methods to a single specimen.

Although no distinct biostratigraphic zone has been established in Sample 1 and Sample 4 to date, the micropaleontologic study disclosed several interesting points. Sample 1 is one of the nodules dredged at the Komabashi Daini Seamount with calcareous ooze which mainly comprises Pliocene calcareous fossils (HARADA *et al.*, 1974). Nuclei of the nodules were dated about 51×10^6 yrs by the fission track dating (NISHIMURA, 1975), and about 38×10^6 yrs by the K-Ar dating (SHIBATA and OKUDA, 1975). However, the nodule is likely to have been formed early-to-middle Pleistocene. This is based upon the observation of calcareous nannoplankton fossils found in the specimen, *i.e.*, the presence of *Coccolithus pelagicus*, *Cyclococcolithina macintyrei* and *Umbilicosphaera mirabilis*, and the absence of members of *Discoaster*, which became extinct at the end of the Pliocene. A recent growth is also implied from the presence of

planktonic foraminiferal assemblage adhering to the nodule surface, consisting exclusively of *Globorotalia menardii*, *G. truncatulinoides*, *G. inflata*, and *Pulleniatina obliquelo-culata*. It is of particular interest to note that the nodule incorporated organic-walled fossils such as pollen grains, spores and scales of butterflies, but no dinoflagellate cysts. This suggests that the nodule was formed under pelagic conditions at the site in early to middle Pleistocene (see HARADA, 1977a), which agrees with the hypothesis that the Philippine Sea deepened from a shallow marginal sea to the present oceanic stage at about two million years ago (IKEBE, 1976).

Sample 4 contained individuals of calcareous nannoplankton fossils instead of impressions. They consisted of *Cyclococcolithina leptopora*, *Pseudoemiliania lacunosa*, and *Gephyrocapsa oceanica*. As *Ps. lacunosa* occurs, the age of the assemblage is assigned to NN 19. The fossils may have been reworked like *Chiasmolithus grandis* in Sample 2. But if they are *in situ* fossils, the surface of the second layer is dated at $0.4–1.6 \times 10^6$ yrs according to BERGGREN and VAN COUVERING (1974, p 34). As the initial age of the outermost layer is younger than this date, the minimum mean growth rate is tentatively calculated to be 0.9–3.8 mm/10^6 yrs. The value is consistent with accretion rates determined radiometrically (see KU, 1977).

Since this study used the standard nannoplankton zones for a time scale, the age of layers was determined with a broad range. However, if we can correlate the sequential change of fossil assemblage in nodule layers to that in a sediment column in the vicinity of the nodule province, more detailed chronologic data will be obtained.

The micropaleontologic study has another advantage. During the course of the Deep Sea Drilling Project (DSDP), buried nodules have been encountered at depth in the drilled cores. CRONAN (1973) first discovered *in situ* buried nodules in a core from the Eastern Pacific. The chemical composition of these nodules was shown to differ from that of Recent nodules in the vicinity of the drilling site. AUMENTO and MACGILLIVRAY (1975) encountered several nodules at different depths in a core from the Antarctic Ocean and estimated the age of nodule formation to be Miocene. They also suggested that the chemical characteristics indicated rapid formation of the nodules followed by rapid burial. More recently, MENARD (1976) analysed the occurrence of buried nodules in DSDP cores from the Pacific. He found that the probability of finding nodules decreases from the Eocene with time, and concluded that nodules probably were more abundant at the sediment surface in Tertiary time than they are now. These buried nodules are a kind of fossil which record oceanic condition at the time of burial. The micropaleontologic study should yield chronologic information for this kind of nodule.

The origin of marine manganese nodules has been widely discussed by ocean scientists. Marine chemists claimed direct precipitation of ferromanganese oxides from sea water (MURRAY and RENARD, 1891; GOLDBERG and ARRHENIUS, 1958; CRERAR and BARNES, 1974; BURNS and BURNS, 1975; NOHARA, 1976), while the marine

biologists stressed the role of microbes in the process of manganese deposition (GRAHAM and COOPER, 1959; EHRLICH, 1963, 1975). Most of the considerations, however, presume very low rates for the nodule accretion of the order of a few millimeters to some centimeters per million years derived from direct measurements (*e.g.*, BENDER *et al.*, 1970; CRERAR and BARNES, 1974). However, these studies have paid little attention to the internal structure of nodules which records the growth history and mechanisms of formation of the nodule.

Significance of the investigation of the internal structure was first pointed out by SOREM (1967). He studied the internal structure by examining polished sections by ore microscope (SOREM, 1973; SOREM, and FOSTER, 1972). This method, however, prevents three dimensional examination of nodule structure. Recent development of SEM techniques has shed a new light on the problem. MARGOLIS and GLASBY (1973) discovered fine laminations in ferromanganese layers of Pacific nodules, and attributed this to the variation of the rates of precipitation of metal oxides which may be governed by variations of bottom currents at the sea floor. FEWKES (1973) examined Pacific nodules, and observed direct crystallization of ferromanganese oxides and non-crystalline deposits of colloidal origin on the nodule surface as well as in the nodule interior. He also suggested the presence of ancient growth surface preserved within nodule crusts. LAROCK and EHRLICH (1975) found *in situ* bacterial colonies on the fresh surface of nodules from the Blake Plateau. More recently, activity of benthic microorganisms has been recognized to be of genetic significance. GREENSLATE (1974a) discovered hollow tubes and domes of encrusting microorganisms on the surface of nodules from the Pacific. He has claimed that some microorganisms are participating in nodule accretion by agglutinating micronodules to the nodule surface when they make their tests, and that siliceous fossils nucleate the micronodules (GREENSLATE, 1974b). WENDT (1974) found that the biogenic structures commonly exist on the surface of Recent nodules, encrustations, and slabs. Examining the internal structure in thin section, he discovered that some parts of the ferromanganese layers were composed of masses of agglutinating foraminifers and assigned values of 0.04–1 mm/yr to the rate of accretion of these parts, assuming a life cycle of the organisms of a half to one year. The association of sessile foraminifers with ferromanganese layers was observed in a nodule from the North Atlantic by SCHAAF *et al.* (1977). They also suggested a rapid accretion of the nodule crust by the paleontologic evidence. DUGOLINSKY *et al.* (1977) examined nodules from the Pacific and recognized 24 species of benthic foraminifers as well as 24 kinds of unidentified protozoans on nodule surface, and the structures produced by these organisms inside. They considered that these protozoans initiate the nodule formation and promote the nodule accretion. Although the rapid growth can account for the abundant occurence of various fossils and internal features of nodules, it is incompatible with the very low rate of accretion established by direct measurement.

Two distinct textures recognized in this study appear to suggest that two kinds of growth mechanisms may operate alternatively in the process of nodule formation, corresponding to environmental change. The fine lamination is considered to result from the direct precipitation of ferromanganese oxides. This mechanism is likely to be favoured by low sedimentation rates which are commonly recognized in most nodule provinces (HORN *et al.*, 1972). The sediment bearing Sample 3 contains a small amount of poorly preserved calcareous nannoplankton fossils whose assemblage indicates NN 19. It suggests a very low rate of deposition since Late Pleistocene, which is confirmed by bottom photographs of the site (GLASBY and SINGLETON, 1975). Assuming that the upper 2 mm of the specimen have been growing by the slow precipitation mechanism since Late Pleistocene, the accumulation rate for this part is estimated at about a few millimeters per million years which is in good agreement with the commonly accepted rate. Likewise the laminated outermost layer of Sample 4 has an accretion rate of the order of a few millimeters per million years, although the value is tentative. On the contrary, the massive texture is infered as a result of some process involving biologic activity. Encrusting organisms initiate it by building a porous framework rapidly, probably with the rate of the order of millimeter per years as suggested by WENDT (1974), using their tests, on a solid substratum, the nucleus of a nodule. In this stage, fossils of planktonic organisms may be incorporated into the framework. The space within the framework is then gradually filled with ferromanganese oxides which may be brought into the space by interstitial water. In this stage, microbes, especially manganese oxidizing bacteria, feeding on organic compounds on the walls of tubes (GRAHAM and COOPER, 1959), are likely to promote the ferromanganese deposition when the amount of organic matter is at optimum (see EHRLICH, 1975). This mechanism inevitably requires high surface productivity which supplies the benthic community with biogenic detritus as food. Detritus also participates in vertical transportation of nodule constituent metals to the ocean floor (ARRHENIUS, 1963; GREENSLATE *et al.*, 1973). The bottom current is necessary for oxygen supply to the ocean floor (BURNS and BURNS, 1972). When the sedimentation is high due to the high surface productivity, the encrusting organisms on the nodule as well as larger benthos in the sediment may keep the nodule at the sediment surface as has been suggested by GREENSLATE (1974a), DUGOLINSKY *et al.* (1977) and MENARD (1976). The variation of the dimension of the framework and constituent tubes, and of the authigenic mineral content in ferromanganese layers of individual nodules, indicates that various kinds of benthic organisms, including agglutinating foraminifers, are able to take part in the construction of the framework, and that nodule accretion by this mechanism occurs intermittently under different conditions. Discontinuous growth has been infered by the rates obtained in Sample 2 (HARADA and NISHIDA, 1976). The presence of the ancient growth surface within nodules suggests a hiatus between ferromanganese layers. This may explain the low growth rate for the whole oxide

Table 4. Chemical composition of the nodules from the Komabashi Daini Seamount and the Southwestern Pacific Basin.

Sample location		Mn	Fe	Cu	Ni	Co	No. of nodules analysed
Komabashi Daini Seamount (G12)[1]		18.2	18.6	0.083	0.42	0.42	6
Southwestern Pacific Basin (G994)[2]	ϕ[3]	17.5	21.8	0.23	0.41	0.48	17
	O.L.[4]	17.8	23.5	0.25	0.44	0.58	2

[1] After USUI *et al.* (1976)
[2] After GLASBY *et al.* (1975)
[3] Average composition of the whole nodule.
[4] Composition of the outer layer.

parts of nodules estimated by the nucleus dating method (see KU, 1977, p. 256). The environmental change, influencing the accretion mechanisms, should be recorded in the sedimentary sequence in the vicinity of the depositional site. It is therefore possible to verify the hypothesis postulated here by examining the sequence, although such data are not available at present.

Although no chemical analysis was performed on these samples, a few data are available on the chemical composition of Sample 1 and Sample 3. USUI *et al.* (1976) carried out petrological, mineralogical and chemical studies on the nodules from the Komabashi Daini Seamount where Sample 1 was collected (G12). The average composition of the nodules is given in Table 4. They distinguished two distinct mineral phases comprising the ferromanganese layers; 10 Å manganite and δ-MnO_2. The 10 Å manganite phase was found to contain microfossils and clastics abundantly under ore microscope, while the latter to show colloform structure containing detrital materials. They considered that 10 Å manganite was rapidly formed in a short period as compared to δ-MnO_2, probably due to the supply of metal elements from interstitial waters of associate sediments, while δ-MnO_2 was formed through low accumulation of colloidal ferromanganese hydroxides incorporating detrital materials. The inference seems to be compatible with the above mentioned hypothesis. GLASBY *et al.* (1975) analysed chemical composition of the nodules from the Southwestern Pacific Basin (G994). Their result, however, seems not to present any conspicuous change in chemical compositions of different parts of the nodules (Table 4). Nevertheless the presence of textural differences within individual nodules requires reasonable explanation on the origin of internal texture.

As mentioned above, the formation of marine manganese nodule associates with several environmental factors, such as sedimentation rate, water movement, surface productivity and activity of benthic community. It is obvious that we have to examine not only the properties of nodule in detail, but also many other subjects which may

yield information on ancient oceanographic conditions. However, no systematic and integral study has been performed on manganese nodules in Japan to date (see HARADA, 1977a), partly because no systematic sampling was possible until the Geological Survey of Japan started the project for manganese nodule exploration in 1974 (see MIZUNO, 1975). Now the systematically collected samples from the Central Pacific Basin as well as many other useful data are available (MIZUNO and CHUJO, 1975). Extensive micropaleontologic investigation on these samples will produce useful informations on both nodule chronology and growth mechanisms. This will lead us to better understanding of their origin, which, in turn, gives rise to a new tool to reconstruct ancient oceanographic condition on the deep-sea floor.

Summary

Acid treatments revealed existense of a large amount of fossils of both planktonic and benthic organisms present in the nodules from the Pacific. The SEM observation confirmed universal presence of microfossils inside of the ferromanganese layers. They are calcareous nannoplankton, diatoms, planktonic foraminifers, radioralians, sponges, unknown benthic microorganisms, and fossil bacterial colonies. Based on nannoplankton assemblages, the rate of accretion of some samples were estimated by a biostratigraphic method. The values indicate very low rate of accumulation of layers of the order of millimeters to some centimeters per million years, which is in good agreement with the rates determined radiometrically.

The SEM observation disclosed two distinct textures in the ferromanganese crust within individual nodules; a finely laminated texture, and a massive and chaotic one. The textural differences become clearer in the hydrochloric acid insoluble residues of nodules. The former appeared to result from the direct precipitation of ferromanganese oxide with very low rate of accumulation under low sedimentation rate, while the latter grows rapidly enough to incorporate many kinds of fossils and authigenic minerals by the aid of encrusting organisms, including sessile foraminifers, under higher productive condition.

If the two growth mechanisms operate alternatively corresponding to environmental change, we can appropriately explain the internal features and abundant occurrence of various fossils. The low accretion rate for the whole oxide parts of nodules given by the nucleus dating method may be well explained by hiatus between layers, which are indicated by the presence of preserved ancient growth surface within nodules.

In order to verify the hypothesis, it is indispensable to study the sedimentary sequence in the vicinity of the nodule sampling sites, because it should record the environmental change which controls nodule formation. Although no such data are available at present, it is desirable to obtain such a sedimentary sequence with nodules to comprehend the origin of nodules.

Acknowledgements

This study was accomplished as a part of the doctoral thesis at Department of Geology and Mineralogy, Kyoto University under the guidance of Professor Tadao KAMEI. I wish to thank Prof. KAMEI for his supervision and encouragement through the work, and Prof. Shiro NISHIDA, Nara University of Education, for his conduction of nannoplankton micropaleontology. I am indebt to Dr. Geoffrey P. GLASBY, New Zealand Oceanographic Institute, who kindly offered me the manganese nodule samples and most fruitful comments on my work. I wish to thank Prof. Kazuo KOBAYASHI and Noriyuki NASU, Ocean Research Institute, the University of Tokyo, who provided me the opportunities to join the GDP-8 Cruise, 1973, and R≠V Hakuho-Maru KH-74-7 Cruise, 1974, respectively.

I also express my sincere thanks to Prof. Teh-Lung KU, University of Southern California, and Dr. Henry L. EHRLICH of Renselaer Polytechnic Institute, for their critical comments and useful suggestions on the manuscript. Gratitude should extend to Dr. Atsuyuki MIZUNO, the Geological Survey of Japan, who provided with the nodule sample, to Dr. Kojiro NAKASEKO, College of General Education of Osaka University, who offered me the laboratory facilities and financial support, Mr. Akira USUI, Department of Natural Resources Development Engineering, the University of Tokyo, for the valuable information on the results of his chemical analyses, and to Mr. Akira NISHIMURA, the Geological Survey of Japan, for his help with the foraminifer identification.

References

ARRHENIUS, G. (1963): Pelagic sediments. In: HILL, M. N. (ed.), *The Sea*, **3**, Wiley-Interscience, New York, pp. 665–727.

AUMENTO, F. and MACGILLIVRAY, J. M. (1975): Geochemistry of buried Miocene-Pleistocene ferromanganese nodules from the Antarctic Ocean. *Initial Rept. DSDP*, **28**, 759–799.

BENDER, M. L., KU, T. L. and BROECKER, W. S. (1970): Accumulation rates of manganese in pelagic sediments and nodules. *Earth Planet. Sci. Lett.*, **8**, 143–148.

BERGGREN, W. A. and VAN COUVERING, J. A. (1974): The Late Neogene. *Palaeogeogr. Palaeoclimatol. Palaeoecol.*, **16**, 1–216.

BURNS, R. G. and BROWN, B. A. (1972): Nucleation and mineralogical controls on the composition of manganese nodules. In: HORN, D. R. (ed.), *Ferromanganese Deposits on the Ocean Floor*, Conference, Arden House, Harriman, N. Y., 20–22 Jan. 1972, Lamont-Doherty Geological Observatory, Columbia University and IDOE-NSF, pp. 51–62.

BURNS, R. G. and BURNS, V. M. (1975): Mechanism for nucleation and growth of manganese nodules, *Nature*, **255**, 130–131.

CRERAR, D. A. and BARNES, H. L. (1974): Deposition of deep-sea manganese nodules. *Geochim. Cosmochim. Acta*, **38**, 270–279.

CRONAN, D. S. (1973): Manganese nodules in sediments cored during Leg 16, Deep Sea Drilling Project. *Initial Rept. DSDP*, **16**, 605–608.

DUDLEY, W. C. (1976): Cementation and iron concentration in Foraminifera on manganese nodules. *Jour. Foram. Res.*, **6**, 202–207.

DUGOLINSKY, B. K., MARGOLIS, S. V. and DUDLEY, W. C. (1977): Biogenic influence on growth of manganese nodules. *Jour. Sediment. Petrol.*, **47**, 428–445.

EHRLICH, H. L. (1963): Bacteriology of manganese nodules 1. Bacterial action on manganese in nodule enrichments. *Appl. Microbiol.*, **11**, 15–19.

EHRLICH, H. L. (1975): The formation of ore in the sedimentary environment of the deep sea with microbial participation: The case for ferromanganese concretions. *Soil Sci.*, **119**, 36–41.

FEWKES, R. H. (1973): External and internal features of marine manganese nodules as seen with the SEM and their implications in nodule origin. In: MORGENSTEIN, M. (ed.), *The origin and Distribution of Manganese Nodules in the Pacific and Prospects for Exploration*, Symposium, Honolulu, Hawaii, 23–25 July 1973, Valdivia Manganese Exploration Group, University of Hawaii and IDOE-NSF, pp. 21–29.

GLASBY, G. P. (ed.) (1977): *Marine Manganese Deposits*, Elsevier, Amsterdam, 523 p.

GLASBY, G. P., BÄCKER, H. and MEYLAN, M. A. (1975): Metal contents of manganese nodules from the Southwestern Pacific Basin, *Erzmetall*, **28**, 340–342.

GLASBY, G. P. and SINGLETON, W. R. (1975): Underwater photographs of manganese nodules from the Southwestern Pacific Basin. *N. Z. Jour. Geol. Geophys.*, **18**, 597–604.

GOLDBERG, E. D. and ARRHENIUS, G. (1958): Geochemistry of Pacific pelagic sediments. *Geochim. Cosmochim. Acta*, **13**, 153–212.

GRAHAM, J. W. and COOPER, S. C. (1959): Biological origin of manganese rich deposits of the sea floor. *Nature*, **138**, 1050–1051.

GREENSLATE, J. L. (1974a): Microorganisms participate in the construction of manganese nodules. *ibid.*, **249**, 181–183.

GREENSLATE, J. L. (1974b): Manganese and biotic debris association in some deep-sea sediments. *Science*, **186**, 529–531.

GREENSLATE, J. L., FRAZER, J. Z. and ARRHENIUS, G. (1973): Origin and deposition of selected transition elements in the seabeds. In: MORGENSTEIN, M. (ed.), *The Origin and Distribution of Manganese Nodules in the Pacific and Prospects for Exploration*, Symposium, Honolulu, Hawaii, 23–25 July 1973, Valdivia Manganese Exploration Group, University of Hawaii and IDOE-NSF, pp. 45–69.

HARADA, K. (1977a): Paleooceanographic investigations of dinoflagellates and marine manganese nodules. Unpublished Doctoral Thesis, Faculty of Science, Kyoto University.

HARADA, K. (1977b): Marine manganese nodules —a review— *Mar. Sci.*, **9**(**6**), 50–69; (**7**), 48–58; (**9**), 59–60. (in Japanese with English abstract).

HARADA, K., KITAZATO, H., NISHIDA, S. and TAKAYAMA, T. (1974): Some micropaleontologic results on the Cruise GDP-8, 1973. *ibid.*, **6**(**8**), 47–50 (in Japanese with English abstract).

HARADA, K. and NISHIDA, S. (1976): Biostratigraphy of some marine manganese nodules. *Nature*, **260**, 770–771.

HIURA, I. (1973): *Butterflies Acrossing the Sea.* Souju Shoboh, Tokyo, 200 p. (in Japanese).

HORN, D. R., HORN, B. M. and DELACH, M. N. (1972): Distribution of ferromanganese deposits in the world ocean. In HORN, D. R. (ed.), *Ferromanganese Deposits on the Ocean Floor*, Conference, Arden House, Harriman, N. Y., 20–22 Jan. 1972, Lament-Doherty Geological Observatory, Columbia Univ. and IDOE-NSF, pp. 9–18.

IKEBE, N. (1976): Neogene geohistory of Japan in relation to the geohistory of the Philippine Sea. *Mar. Sci.*, **8**(**3**), 24–29 (in Japanese with English abstract).

KU, T. L. (1977): Rates of accretion. In: GLASBY, G. P. (ed.), *Marine Manganese Deposits*, Elsevier, Amsterdam, pp. 249–267.

LAROCK, P. A. and EHRLICH, H. L. (1975): Observation of bacteria microcolonies on the surface of ferromanganese nodules from Blake Plateau by scanning electron microscopy. *Microbial Ecology*, **2**, 84–96.

MARGOLIS, S. V. and GLASBY, G. P. (1973): Microlaminations in marine manganese nodules as revealed

by scanning electron microscopy. *Geol. Soc. Amer. Bull.*, **84**, 3601–3610.

MARTINI, E. and WORSLEY, T. (1970): Standard calcareous nannoplankton zonation. *Nature*, **225**, 289–290.

MENARD, H. W. (1976): Time, change, and the origin of manganese nodules. *Amer. Scientist*, **64**, 519–529.

MEYLAN, M. A., BÄCKER, H. and GLASBY, G. P. (1975): Manganese nodule investigations in the Southwestern Pacific Basin, 1974. *NZOI Oceanogr. Field Rept.*, no. 4, 24 p.

MIZUNO, A. (1975): On the manganese nodule exploration by the Geological Survey of Japan. *Abstracts with Programs*, **82***nd Ann. Meeting, Geol. Soc. Japan*, 1–3 April 1975, Kyoto, p. 379 (abstract, in Japanese).

MIZUNO, A. and CHUJO, J. (eds.) (1975): *Deep Sea Mineral Resources Investigation in the Eastern Central Pacific Basin, August-October* **1974** (*GH***74-5** *Cruise*), Cruise Rept., no. 4, Geol. Surv. Japan, 103 p.

MURRAY, J. and RENARD, A. F. (1891): Manganese nodules. In: THOMSON, C. W. (ed.), *Report of the Scientific Results of the Voyage of the HMS Challenger*, **5**, Deep-Sea Deposits, Eyre and Spottiswoode, London, pp. 341–378.

NASU, N. (ed.) (1978): *Preliminary Report on the R/V Hakuho-Maru Cruise KH-***74-4, 1974. Ocean Res. Institute, University of Tokyo (in press).

NISHIMURA, S. (1975): Fission track dating of a granitic nucleus of manganese nodule from the Komabashi Daini Seamount. In: NAKAZAWA, K. *et al.* (eds.), *Geological Problems of the Philippine Sea*, Geol. Soc. Japan, p. 104 (in Japanese).

NOHARA, M. (1976): A theoretical model for the mechanism of formation of ferromanganese nodules. *Jour. Geol. Soc. Japan*, **82**, 675–686.

SCHAAF, A., HOFFERT, M., KARPOFF, A.-M. and WIRRMANN, D. (1977): Association de structures stromatolithiques et de foraminifères sessiles dans un encroûtement ferromanganésifère á cœur granitique en provenance de l'Atlantique nord. *C. R. Acad. Sc., Paris*, **284D**, 1705–1708.

SHIBATA, K. and OKUDA, Y. (1975): K-Ar age of a granite fragment dredged from the 2nd Komabashi Seamount. *Bull. Geol. Surv. Japan*, **26**, 71–72 (in Japanese with English abstract).

SHIKI, T., AOKI, H., SUZUKI, H., MUSASHINO, M. and OKUDA, Y. (1974): Geological and petrographical results of the GDP-8th Cruise in the Philippine Sea. *Mar. Sci.*, **6**(**8**), 51–56 (in Japanese with English abstract).

SOREM, R. K. (1967): Manganese nodules: Nature and significance of internal structure. *Econ. Geol.*, **62**, 141–147.

SOREM, R. K. (1973): Manganese nodules as indicator of long-term variations in sea floor environment. In: MORGENSTEIN, M. (ed.), *The Origin and Distribution of Manganese Nodules in the Pacific and Prospects for Exploration*, Symposium, Honolulu, Hawaii, 23–25 July 1973, Valdivia Manganese Exploration Group, University of Hawaii and IDOE-NSF, pp. 151–164.

SOREM, R. K. and FOSTER, A. R. (1972): Internal structure of manganese nodules as implications in benefication. In: HORN, D. R. (ed.), *Ferromanganese Deposits on the Ocean Floor*, Conference, Arden House, Harriman, N. Y., 20–22 January 1972, Lamont-Doherty Geological Observatory, Columbia University and IDOE-NSF, pp. 167–182.

USUI, A., TAKENOUCHI, S. and SHOJI, T. (1976): Distribution of metal elements in manganese nodules and formation mechanism of constituent minerals, with special reference to nodules from Komabashi Daini Seamount. *Mining Geol.*, **26**, 371–384 (in Japanese with English summary).

WENDT, J. (1974): Encrusting organisms in deep-sea nodules. *Spec. Publs. Int. Ass. Sediment.*, **1**, 437–447.

Explanation of Plate 3

All the figures are scanning electron micrographs.*

Figure **a**: Enlarged view of the inside of Sample 1. Many calcareous nannoplankton fossils are preserved as impressions. They provide chronologic information on the nodule. Scale bar on the photograph indicates 5 μm.

Figure **b**: Impressions of nannofossils, probably *Coccolithus pelagicus* (WALLICH) SCHILLER. Scale 2 μm.

Figure **c**: Another part of Sample 1. Several kinds of impressions of microfossils are recognized. Scale 10 μm.

Figure **d**: Impression of nannofossils, probably *Cyclococcolithina macintyrei* BUKRY *et* BRAMLETTE, preserved in the matrix of micro-crystals which are tentatively identified as birnessite. Scale 5 μm.

Figure **e**: Impression of nannofossil, probably of *C. pelagicus*. Scale 2 μm.

Figure **f**: Impression of nannofossil preserved in the matrix which appears to be composed of clay. Scale 2 μm.

Figure **g**: A colony of microparticles within Sample 1. Scale 2 μm.

Figure **h**: Enlarged view of Fig. g. The particles are replaced by granular crystals which compose the matrix. It proves that they are a primary feature. Scale 2 μm.

Explanation of Plate 4

All the figures are scanning electron micrographs.

Figure **a**: Scale of butterfly extracted from inside of Sample 1. This type of scales were most common in the assemblage. Scale bar on the photograph indicates 40 μm.

Figure **b**: Detail of the scale suggests that they are not fresh scales, but fossil ones preserved inside of the nodule. Scale 20 μm.

Figure **c**: Another type of scale from Sample 1. Scale 40 μm.

Figure **d**: Another example from the same sample. This type is also common. The abundant occurrence of these scales may suggest a rapid growth of the nodule. Scale 20 μm.

Figure **e**: Botryoidal surface of a layer within Sample 1. It appears to be a preserved ancient growth surface. Scale 200 μm.

Figure **f**: Inner mould of a planktonic foraminiferal test embedded in Sample 1. They are usually composed of clay. Scale 40 μm.

Figure **g**: Impression of planktonic foraminiferal test found on the ancient growth surface as seen in fig. **e**. Scale 40 μm.

Figure **h**: Altered shell of planktonic foraminifer preserved in Sample 2. As specific identification is impossible on these fossils, no chronologic data is obtained. Scale 40 μm.

Explanation of Plate 5

All the figures are scanning electron micrographs.

Figure **a**: Hollow tube of encrusting organism on surface of Sample 2. Scale bar on the photograph indicates 100 μm.

Figure **b**: Detail of the tube. The outer wall is composed of Recent calcareous nannofossils. Scale 5 μm.

Figure **c**: A benthic foraminifer on the surface of Sample 2. Scale 200 μm.

Figure **d**: Calcareous nannofossils adhering to the surface of the same sample consist exclusively of Recent species. Scale 5 μm.

---

* All the scanning electron micrographs, except Pl. 4, figs. **a-d** were taken by HITACHI HSM-2B SEM at 20 kv. Figures **a–d** of Pl. 4 by HITACHI-Akashi Minisem SEM at 15 kv.

Figure **e**: Impression of nannofossils preserved within Sample 2. They are identified as *Cyclococcolithina leptopora* (MURRAY *et* BLACKMAN) KAMPTNER (left), and *Cycl. macintyrei* (right). Scale 2 μm.
Figure **f**: Impressions of *Cycl. leptopora*. This may be a part of a coccosphere. Scale 2 μm.
Figure **g**: Several individuals of *Chiasmolithus grandis* HAY, MOHLER *et* WADE, an Eocene index fossil, in a cavity within Sample 2. They appear to result from reworking of the sediment. Scale 20 μm.
Figure **h**: Detail of the inner structure of Sample 2. Microfossils are generally preserved in the part with massive chaotic texture, and almost absent in that with dense laminated texture. Scale 20 μm.

Explanation of Plate 6

All the figures, except fig. **a**, are scanning electron micrographs.
Figure **a**: Photomicrograph of botryoidal surface of Sample 3. Scale bar on the photograph indicates 1 mm. Photo by Y. OKAZAKI.
Figure **b**: Scanning electron micrograph of the botryoidal surface of the same sample. Scale 200 μm.
Figure **c**: A broken hollow tube on the surface of Sample 3. Scale 200 μm.
Figure **d**: Partly dissolved diatom frustule on the surface of Sample 3. The sediment on the surface is almost free from calcareous fossils. Scale 10 μm.
Figure **e**: Filamentous objects on the surface of Sample 3. They are apparently not attached contaminants. Scale 50 μm.
Figure **f**: Detail of the filament indicates that it is composed of organic material. Scale 10 μm.
Figure **g**: Enlarged view of the botryoids comprising the surface of Sample 3. They are covered with small knobs. Scale 50 μm.
Figure **h**: The small knobs appear to be gathered to form a plane on the botryoid surface. Scale 10 μm.

Explanation of Plate 7

All the figures are scanning electron micrographs.
Figure **a**: Detailed view of the knobs, covering the botryoid surface, suggests their spiral growth. Scale bar on the photograph indicates 2 μm.
Figure **b**: Tangential section of botryoid shows the process that the lamella is formed by aggregation of the small knobs. Scale 10 μm.
Figure **c**: Tangential section of botryoid. Obscure laminations are observed inside of the botryoid (left). Scale 10 μm.
Figure **d**: Enlarged view of fig. **c** presents the growing process of the microlamination. Scale 10 μm.
Figure **e**: Laminated structure of the outermost layer of Sample 3. The sediment covers the surface (top). Scale 50 μm.
Figure **f**: Detail of the microlaminations. Scale 2 μm.
Figure **g**: Botryoidal surface within Sample 3. Note the similarity to the surface texture observed in Sample 1 (Plate 4 fig. **e**). Scale 100 μm.
Figure **h**: Broken hollow tubes on the surface as seen in fig. **g**. Scale 100 μm.

Explanation of Plate 8

All the figures are scanning electron micrographs.
Figure **a**: Section of the second layer of Sample 3. The upper part (right) shows dense laminated texture, while the lower (left) massive and chaotic one. Scale bar on the photograph indicates 500 μm.
Figure **b**: Enlarged view of the lower part of the layer. Tabular structure in the center appears to result from biologic activity. Scale 50 μm.
Figure **c**: Fossil of unidentified benthic microorganism preserved within a lower part of the second layer

of Sample 3. Scale 2 μm.

Figure **d**: Authigenic minerals growing inside of cavity in the layer. They may be crystals of zeolites, as they exist even in acid insoluble residue of the layer. Scale 10 μm.

Figure **e**: Detail of the inner structure of the benthic microorganism of fig. **c**. Similar texture was discovered within Sample 1. Scale 2 μm.

Figure **f**: Similar texture found in another part of the layer. Scale 10 μm.

Figure **g**: Colony of small particles within Sample 3. Scale 50 μm.

Figure **h**: Enlarged view of fig. **g** suggests that the particles relate to biologic activity. Scale 10 μm.

Explanation of Plate 9

All the figures, except figs. **a** and **b**, are scanning electron micrographs.

Figure **a**: Photomicrograph of white acid insoluble residue of the outermost layer of Sample 3. It retains the original surface features (cf. Pl. 6, fig. **a**). Scale bar on the photograph indicates 1 mm. Photo by Y. OKAZAKI.

Figure **b**: Photomicrograph of acid insoluble residue of the innermost layer of the same sample. It shows very porous texture, different from the original one (cf. Pl. 8, Fig. b). Scale 1 mm. Photo by Y. OKAZAKI.

Figure **c**: Scanning electron micrograph of the residue of the outermost layer. Scale 500 μm.

Figure **d**: Enlarged view of the residue of the intermediate layer. Note the textural difference. Scale 500 μm.

Figure **e**: Detailed view of fig. **c**. Texture is massive, and no trace of biologic activity is noticeable. Scale 200 μm.

Figure **f**: Enlarged view of fig. **d**. The porous texture appears to result from biologic activity. Scale 200 μm.

Figure **g**: The residue of the outermost layer shows an organic filament observed in Pl. 5, fig. **c**. Scale 20 μm.

Figure **h**: Detailed view of the hole in fig. **f**. Smooth lining of the hole suggests biologic origin. Scale 50 μm.

Explanation of Plate 10

All the figures are scanning electron photomicrographs.

Figure **a**: The acid insoluble residue of the surface of the intermediate layer of Sample 3, also shows massive texture. Scale on the photograph indicates 500 μm.

Figure **b**: Detail of fig. **a** indicates no biologic activity. Scale 100 μm.

Figure **c**: Microfossils preserved in acid residue of the layer. Scale 100 μm.

Figure **d**: Another part of the residue. A case of a planktonic foraminifer (?) is observed in the center. Scale 100 μm.

Figure **e**: Porous acid residue of the innermost layer of the same sample. Scale 500 μm.

Figure **f**: Detailed view of fig. **e**. The residue is composed of various kinds of hollow tubes. Scale 100 μm.

Figure **g**: Authigenic crystals, probably zeolites, in the residue. They appear to be incorporated into the layer by tubes of encrusting organisms. Scale 100 μm.

Figure **h**: Enlarged view of the tube in fig. **g**. The outer wall is composed of well sorted grains, differing from the matrix sediment. It proves that the tubes are biogenic. Scale 10 μm.

Explanation of Plate 11

All the figures are scanning electron micrographs.

Figure **a**: Broken tube on the surface of Sample 4. Scale bar on the photograph indicates 100 μm.
Figure **b**: The sediment covering the surface consists of Recent calcareous nannofossils and fragments of diatoms and radiolarians. Scale 10 μm.
Figure **c**: Section of the outermost layer of Sample 4. Scale 100 μm.
Figure **d**: High magnification view of the outermost layer shows the similar knobby texture to those observed in Sample 3 (Pl. 7, figs. **b, c, d**). Scale 5 μm.
Figure **e**: Concave bottom surface of the outermost layer. Scale 100 μm.
Figure **f**: Impressions of calcareous nannofossils and diatoms preserved on the bottom surface of the layer. Scale 5 μm.
Figure **g**: Ridge-like structure observed on the bottom surface of the layer. This structure is commonly found in all the samples. Scale 20 μm.
Figure **h**: Detail of the ridge appears to consist of organic material. This may be a part of tests of encrusting organisms. Scale 5 μm.

Explanation of Plate 12

All the figures are scanning electron micrographs.
Figure **a**: Section of the second layer of Sample 4. The upper part (left) is massive, and the lower (right) shows many ridge-like structures and cavities. Scale bar on the photograph indicates 500 μm.
Figure **b**: Enlarged view of the lower part of the layer. Scale 200 μm.
Figure **c**: Detail of the upper part of the layer. It shows granular and layering texture, and lacks ridge-like structure. Scale 200 μm.
Figure **d**: High magnification view of the upper part of the layer reveals that the granular texture consists of assemblage of small particles. Scale 20 μm.
Figure **e**: Detail of fig. **d**. The particles are agglutinated with membraneous material. It suggests that they may be a fossilized bacteria colony. Scale 2 μm.
Figure **f**: High magnification view of the particles. They are replaced by microcrystals like those observed in Sample 1 (Pl. 3, fig. **h**). Scale 2 μm.
Figure **g**: Enlarged view of the surface of the second layer of Sample 4. Scale 20 μm.
Figure **h**: Low magnification view of botryoidal surface of the layer. Scale 200 μm.

Explanation of Plate 13

All the figures are scanning electron micrographs.
Figure **a**: *Cyclococcolithina leptopora* (MURRAY *et* BLACKMAN) KAMPTNER on the surface of the second layer of Sample 4. Scale bar on the photograph indicates 2 μm.
Figure **b**: Sediment covering the surface consists of both calcareous and siliceous fossils. Scale 10 μm.
Figure **c**: Acid insoluble residue of the outermost layer of Sample 4 shows massive texture. Scale 500 μm.
Figure **d**: Detail of the residue indicates no biologic activity. Scale 100 μm.
Figure **e**: The residue of the second layer of the same sample exhibits very porous texture. Scale 500 μm.
Figure **f**: Enlarged view of the residue shows broken tubes with smooth lining. Scale 100 μm.
Figure **g**: Detail of the broken tube seen in fig. **f**. Scale 10 μm.
Figure **h**: High mangification view reveals that the smooth lining of the tube consists of small plates, which seem to be composed of organic material, since they withstand the hydrochloric acid treatment. Scale 5 μm.

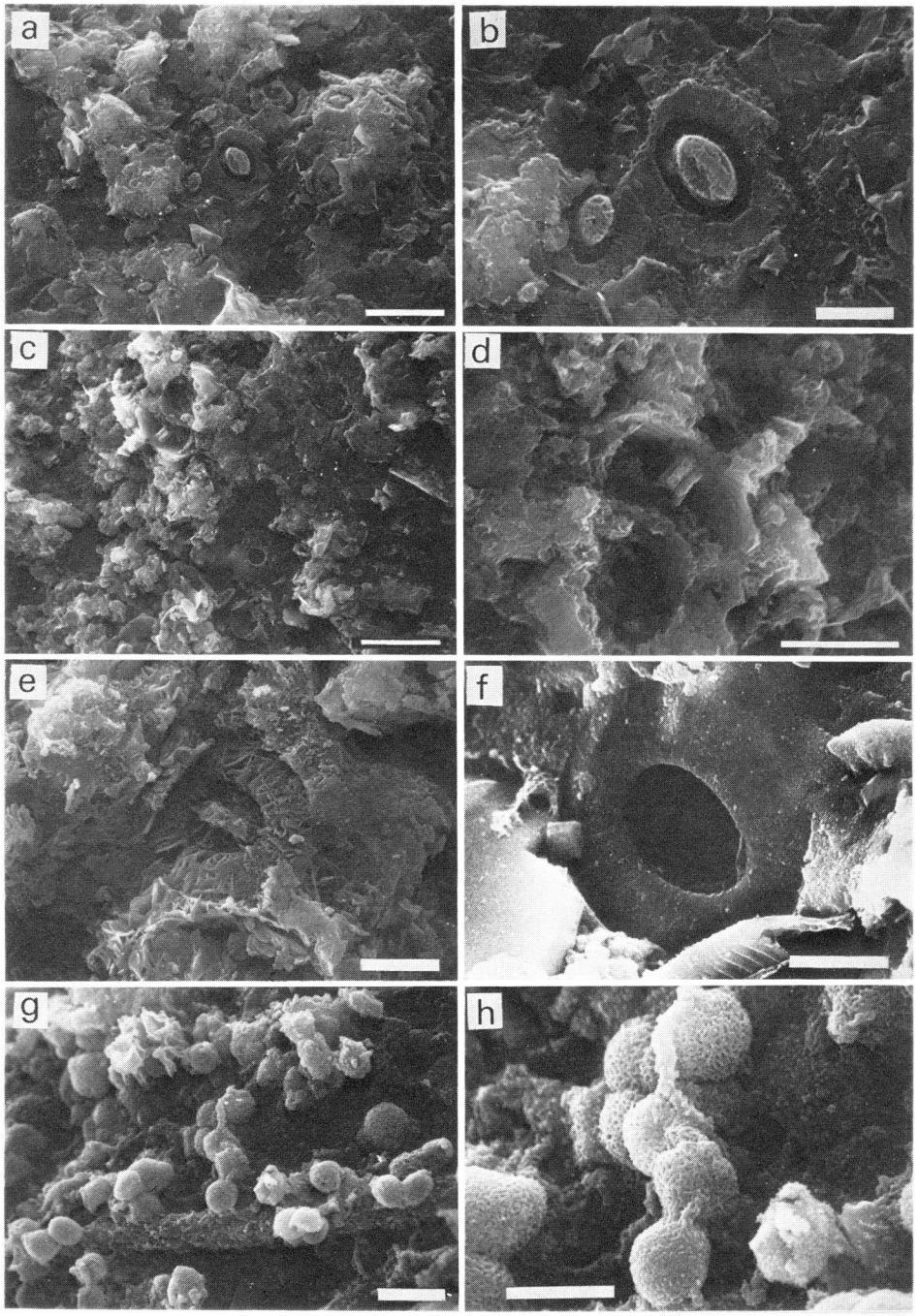

HARADA: Micropaleontology of Mn-Nodules

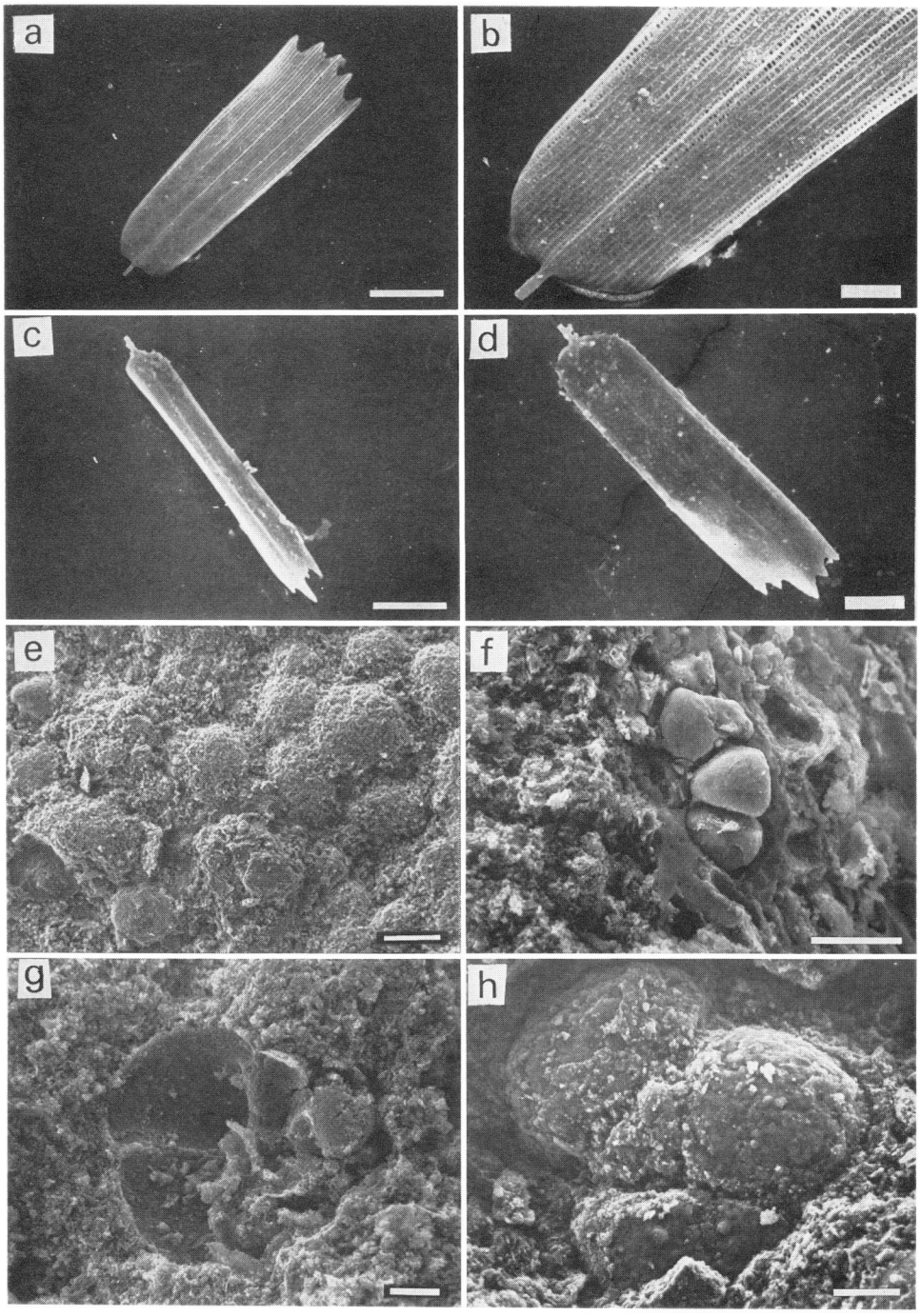
a
b
c
d
e
f
g
h

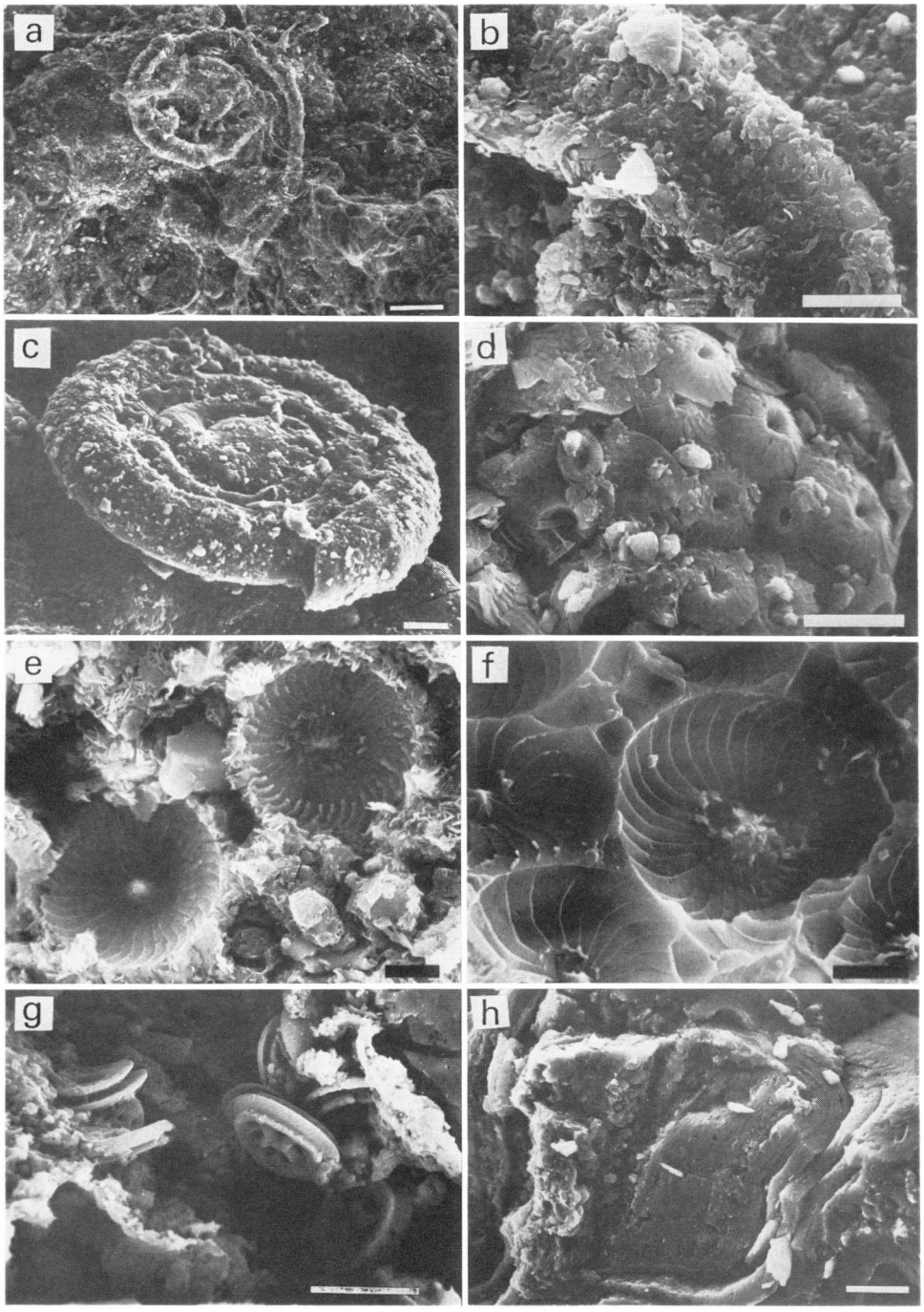

HARADA: Micropaleontology of Mn-Nodules

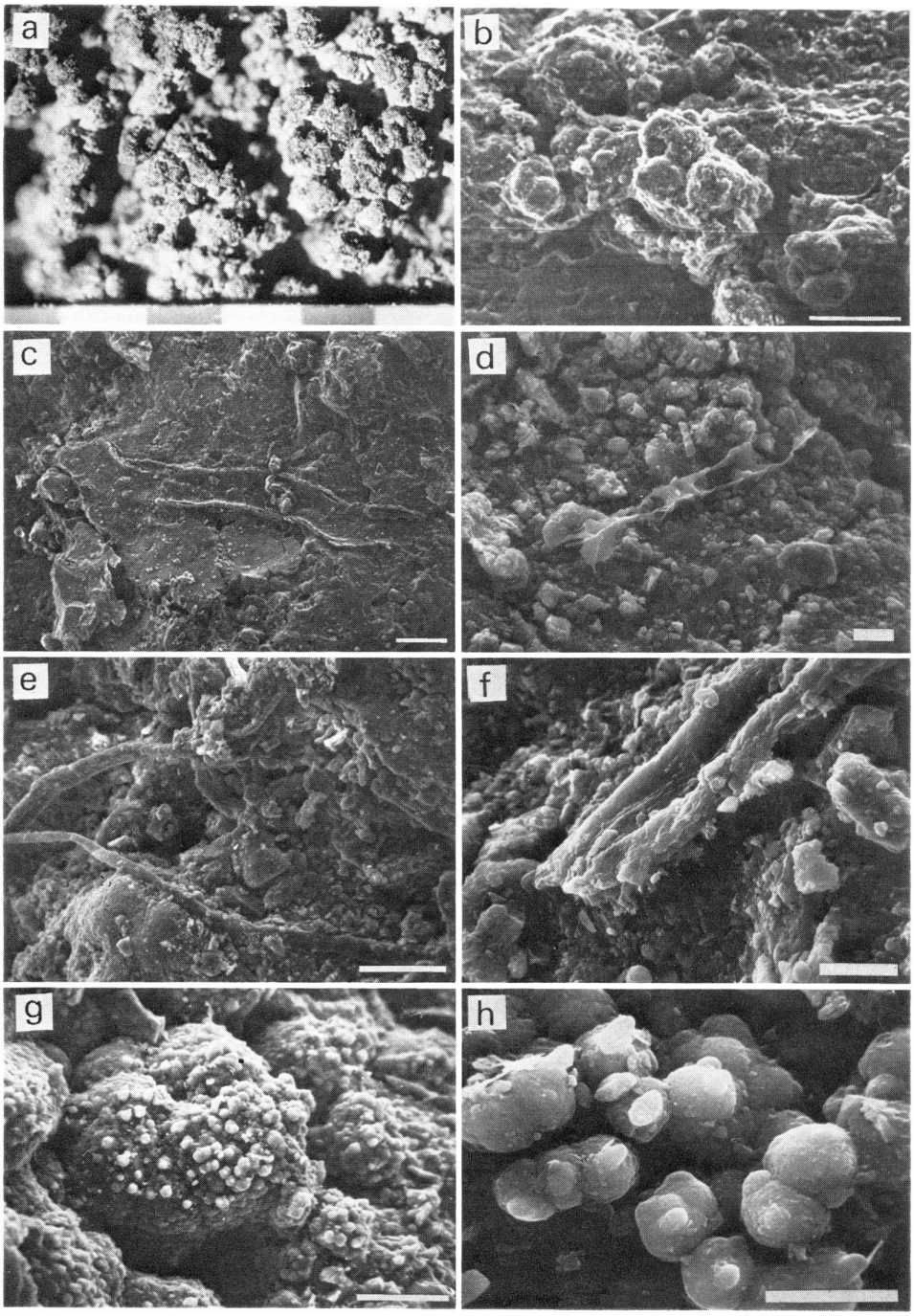

HARADA: Micropaleontology of Mn-Nodules

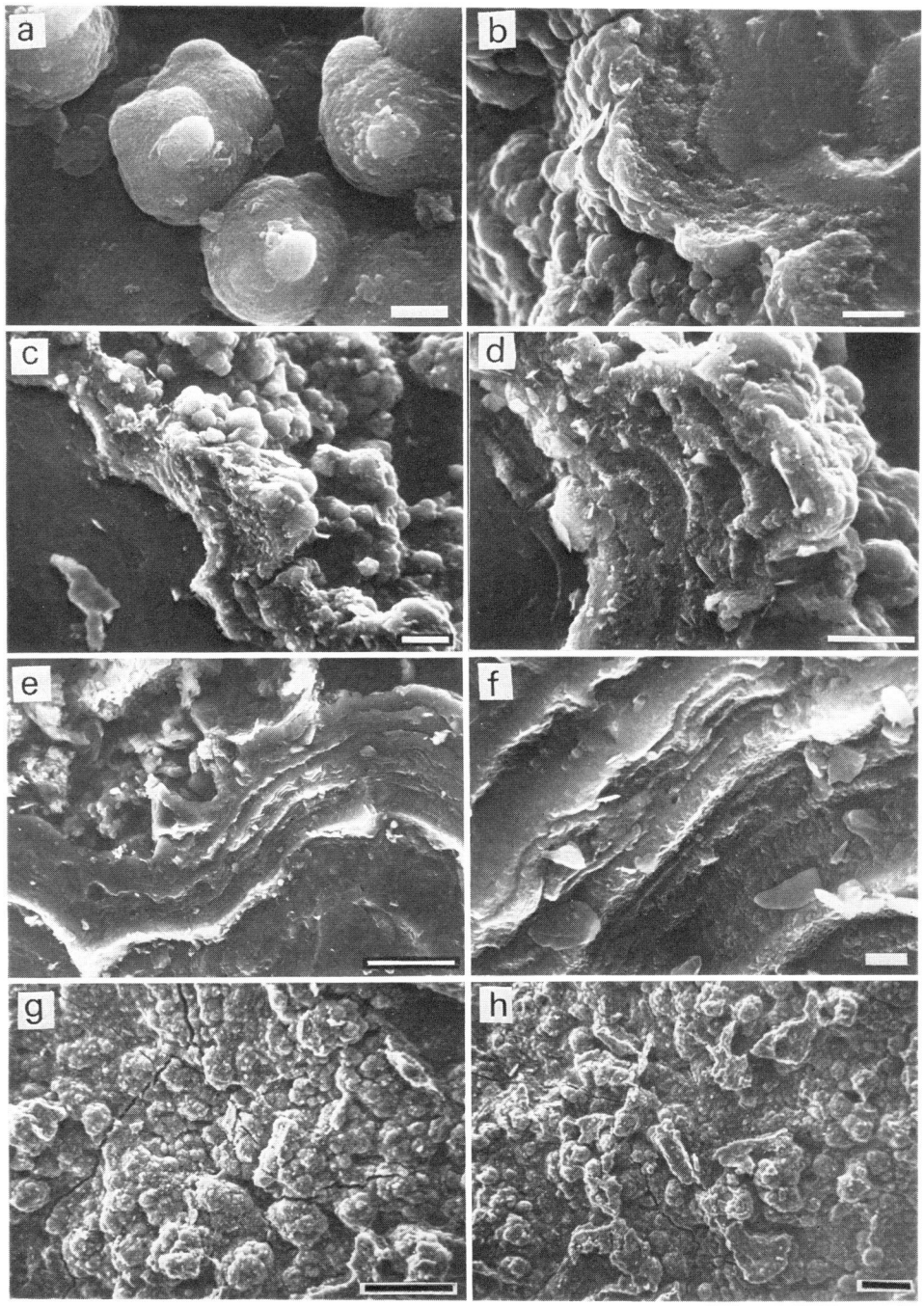

HARADA: Micropaleontology of Mn-Nodules

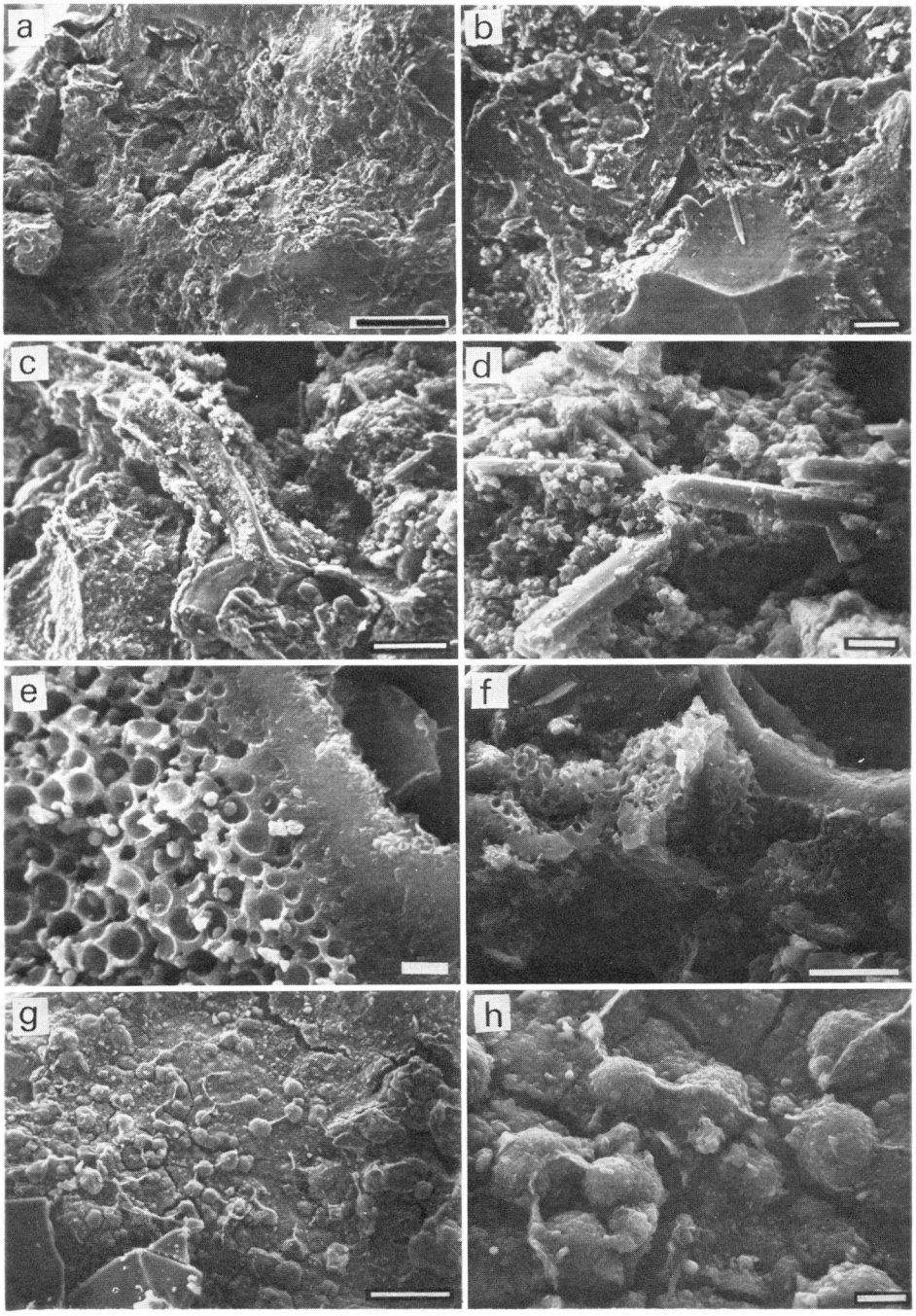
a
b
c
d
e
f
g
h

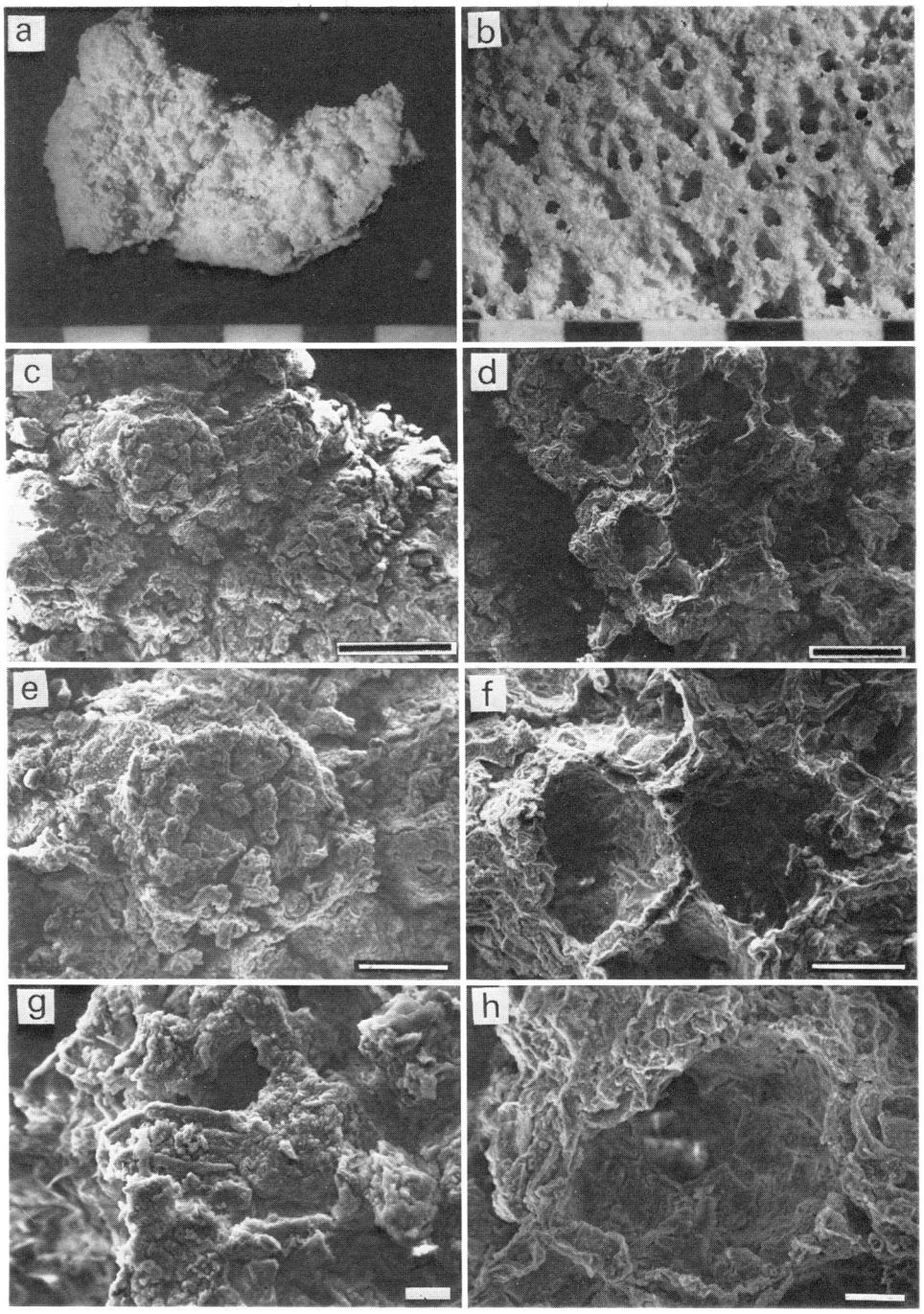
a
b
c
d
e
f
g
h

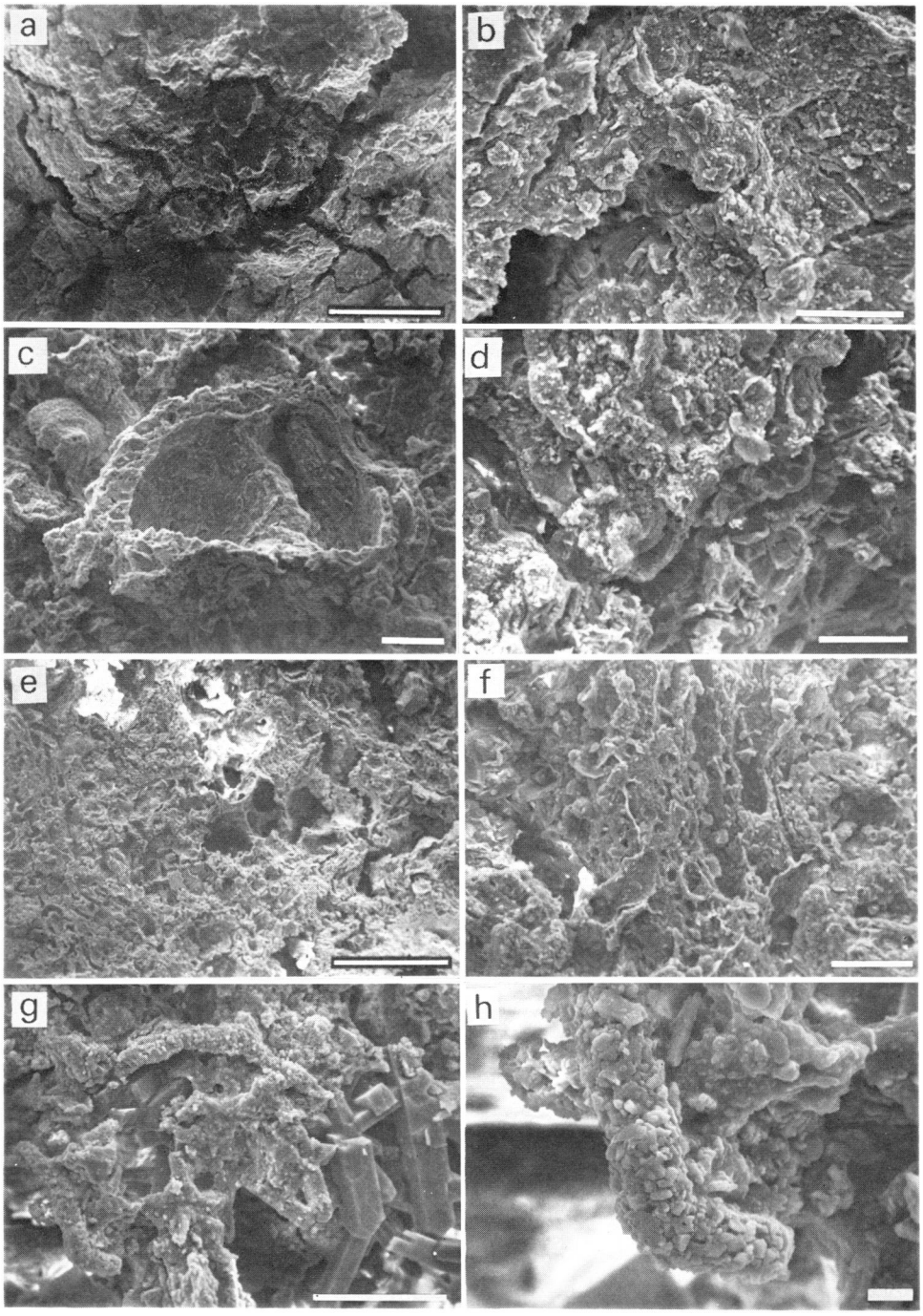
a
b
c
d
e
f
g
h

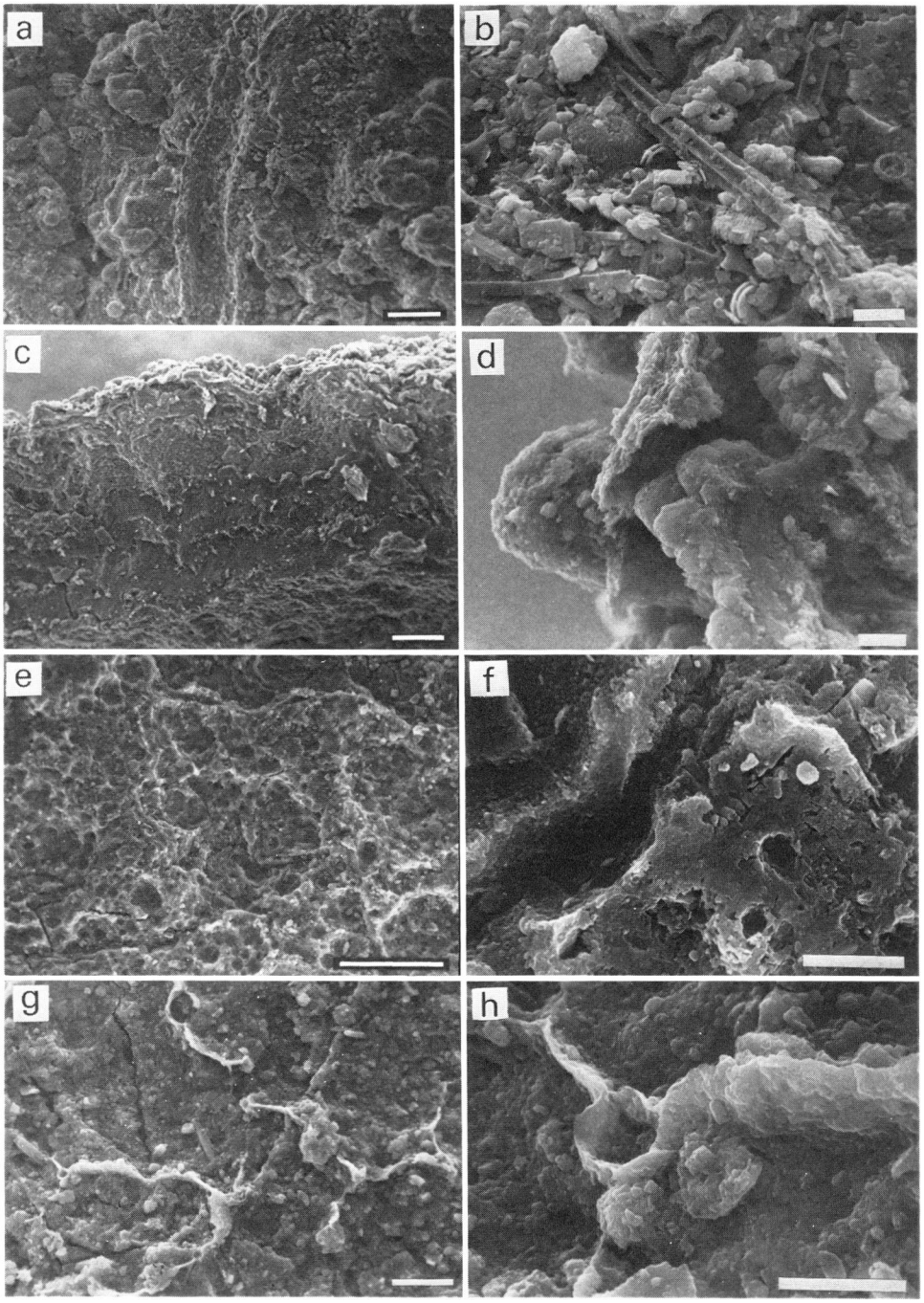

HARADA: Micropaleontology of Mn-Nodules

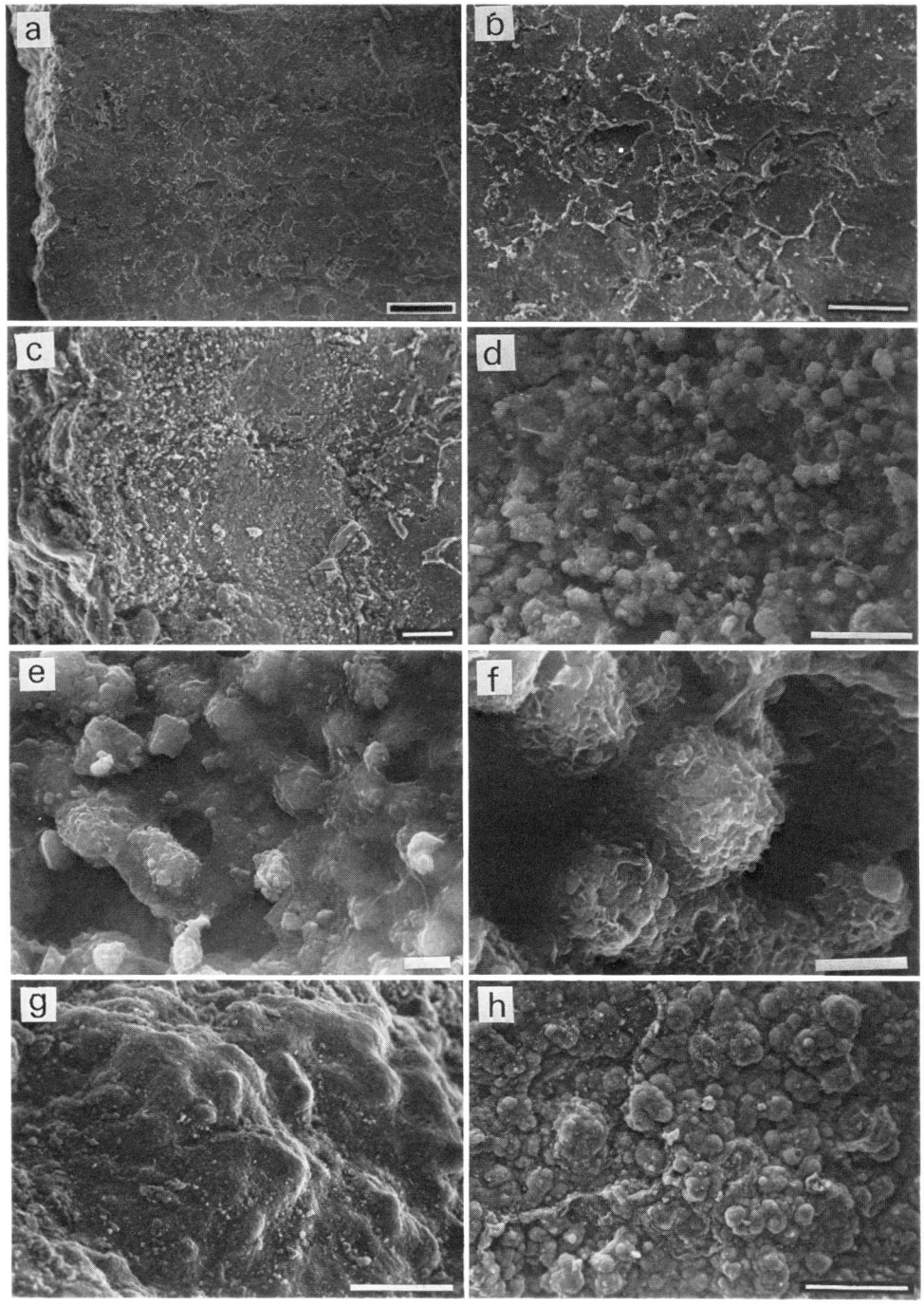
a
b
c
d
e
f
g
h

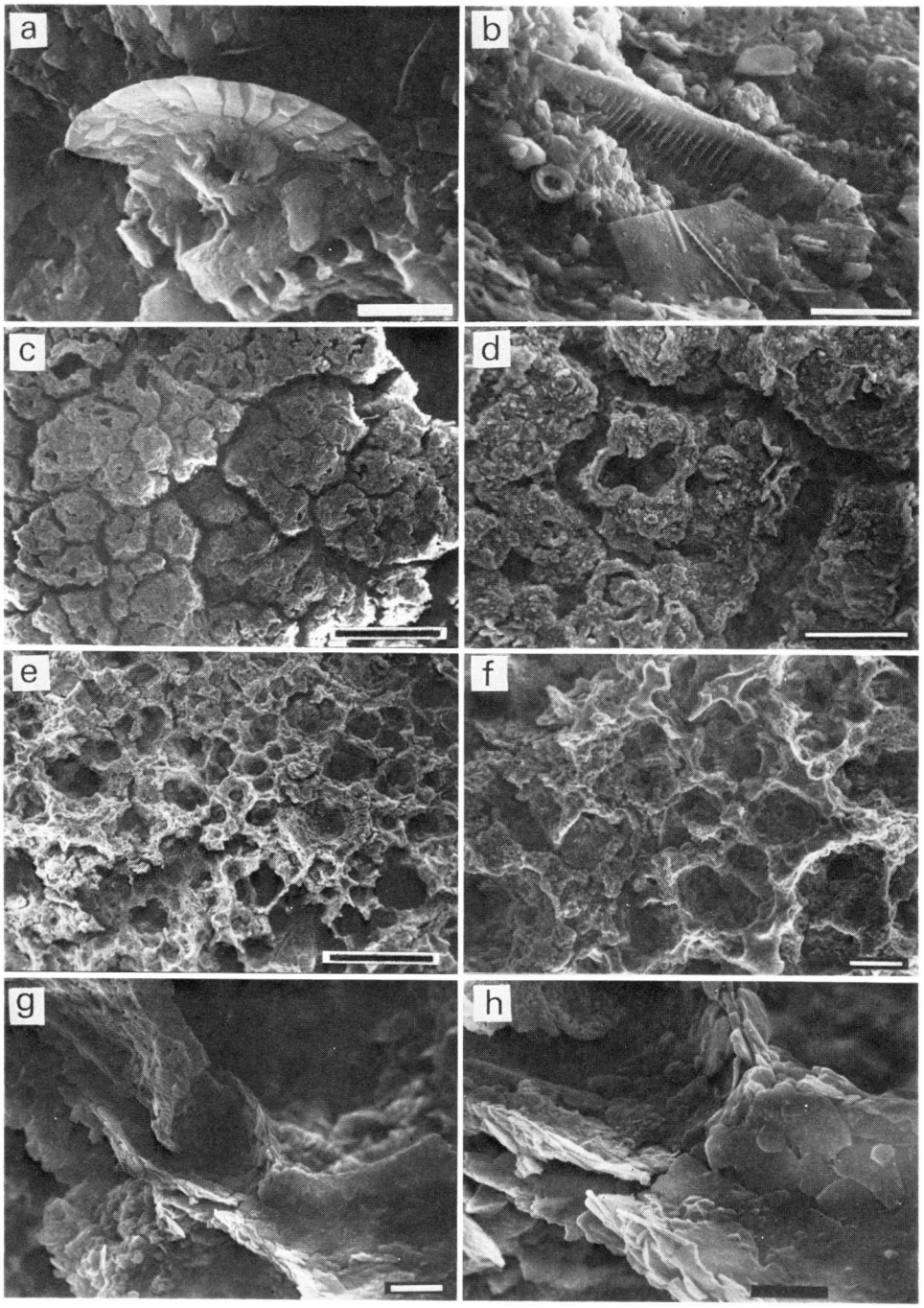
a
b
c
d
e
f
g
h